Ore Geology Reviews 84 (2017) 338–346

Contents lists available at ScienceDirect

Ore Geology Reviews

journal homepage: www.elsevier.com/locate/oregeo

New precise zircon U-Pb and muscovite ^{40}Ar-^{39}Ar geochronology of the Late Cretaceous W-Sn mineralization in the Shanhu orefield, South China

Yongfeng Cai [a,*], Zuohai Feng [a,*], Tongbin Shao [b], Rongguo Hu [a], Yun Zhou [a], Jifeng Xu [b]

[a] Collaborative Innovation Center for Exploration of Hidden Nonferrous Metal Deposits and Development of New Materials in Guangxi & Guangxi Key Laboratory of Hidden Metallic Ore Deposits Exploration, Guilin University of Technology, Guilin 541004, China
[b] State Key Laboratory of Isotope Geochemistry, Guangzhou Institute of Geochemistry, Chinese Academy of Sciences, Guangzhou 510640, China

ARTICLE INFO

Article history:
Received 10 September 2016
Received in revised form 14 January 2017
Accepted 23 January 2017
Available online 25 January 2017

Keywords:
Zircon U-Pb dating
Muscovite $^{40}Ar/^{39}Ar$ dating
Shanhu W-Sn deposit
Nanling region

ABSTRACT

The Shanhu orefield, located in the northeastern Guangxi province, is an important part of W-Sn polymetallic metallogeny in the Nanling region. The Shanhu W-Sn deposit is spatially associated with the Yantianling granite. LA-ICPMS zircon U-Pb dating of the Yantianling granite yields Late Cretaceous ages of 100.9 ± 2.2 Ma and 100.8 ± 2.3 Ma. Hydrothermal muscovite $^{40}Ar/^{39}Ar$ dating yields plateau ages of 102.7 ± 1.7 Ma and 100.8 ± 0.7 Ma. This date coincides well with the LA-ICPMS zircon U-Pb age of the Yantianling granite, indicating a spatial-temporal link between the W-Sn mineralization and the granitic magmatism. In combination with regional geological data, it is suggested that a Late Cretaceous mineralization event related to granitic magmatism occurred in the Nanling region, which might have resulted from regional lithospheric extension.

1. Introduction

The South China Craton formed by the amalgamation of Yangtze and Cathaysia blocks along the Jiangnan belt in the Neoproterozoic (Cai et al., 2014, 2015), and was modified by the following Paleozoic and Mesozoic tectonic events (e.g., Zhou et al., 2015a,b,c). These events resulted in large volumes of granitic rocks, associated with W, Sn, Cu, Bi, Mo, Pb and Zn mineral systems throughout South China (Fig. 1; e.g., Mao et al., 2013). Previous studies have shown that large-scale W-Sn polymetallic mineralization in South China occurred mainly at 160–150 Ma, and there is no distinct time interval between W-Sn mineralization and its intimately associated granitic magmatism (Feng et al., 2015). Recent studies have identified a Late Cretaceous metallogenic event in southwestern and southeastern China and adjacent areas, such as the world famous Gejiu and Dachang skarn-type tin deposits and the Zijinshan porphyry-epithermal Cu-Au system in south Yunnan, Guangxi, and Fujian provinces, respectively (Cheng et al., 2013; Yuan et al., 2015; Mao et al., 2013). To date, however, little evidence of Late Cretaceous W-Sn mineralization has been reported in the Nanling region.

In this paper, new precise zircon U-Pb and muscovite Ar-Ar isotopic dating have been performed on the granites and associated tungsten-tin ore samples from the Shanhu orefield, respectively. Combined with regional geological data, the geochemical results are used to constrain the possible link between Late Cretaceous tungsten-tin mineralization and the Shanhu orefield, by means of (1) determining the timing of granite, (2) the ore-forming age of the Shanhu orefield, and (3) discussing the spatial-temporal relationship between the granite and mineralization.

2. Geological background

The mountainous Nanling region, covers an area of about 170,000 km^2, is located at the intersection of Guangxi, Guangdong, Jiangxi and Hunan provinces (Fig. 1) (Chen et al., 2002; Yuan et al., 2011). The Nanling region lies in the northwestern part of the Cathaysia Block. The region is an important W-Sn polymetallic metallogenic province with quartz-vein type tungsten deposits in the east and skarn-type W-Sn polymetallic deposits in the west (Yuan et al., 2015).

The Shanhu orefield is located in the northwest of the Nanling region, South China (Figs. 1 and 2). Cambrian basement and Devonian-Cretaceous sedimentary cover are wide distributed in the region (Fig. 3). The exposed rocks in the orefield are of Devonian age divided, from the base to top, into the Lianhuashan, Nagaoling, Yujiang, Donggangling, Guilin, and Rongxian formations (Fig. 3).

Folds and faults are well developed in the region with the main tectonic line trending NNE (Fig. 2). Mesozoic granites are widely

* Corresponding authors at: College of Earth Sciences, Guilin University of Technology, No. 12, Jiangan Road, Guilin 541004, China.
E-mail addresses: caiyongfeng@glut.edu.cn (Y. Cai), fzh@glut.edu.cn (Z. Feng).

http://dx.doi.org/10.1016/j.oregeorev.2017.01.022
0169-1368/

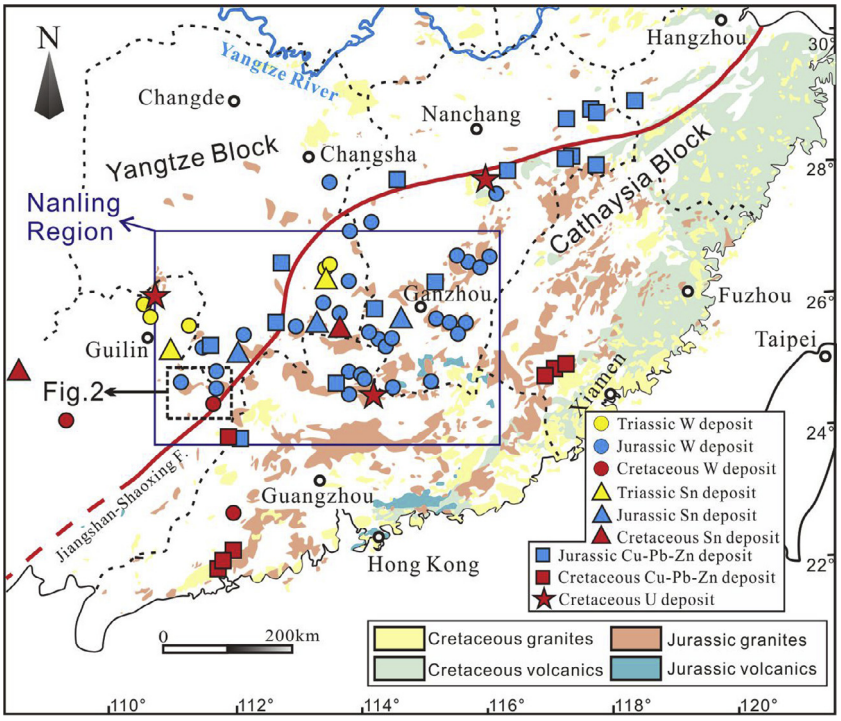

Fig. 1. Simplified geotectonic map showing the Mesozoic igneous rocks and related W-Sn-Cu-Pb-Zn-Mo ore deposits in South China (modified after Zhou et al., 2015a). The age data are from Supplementary Tables S3–S5.

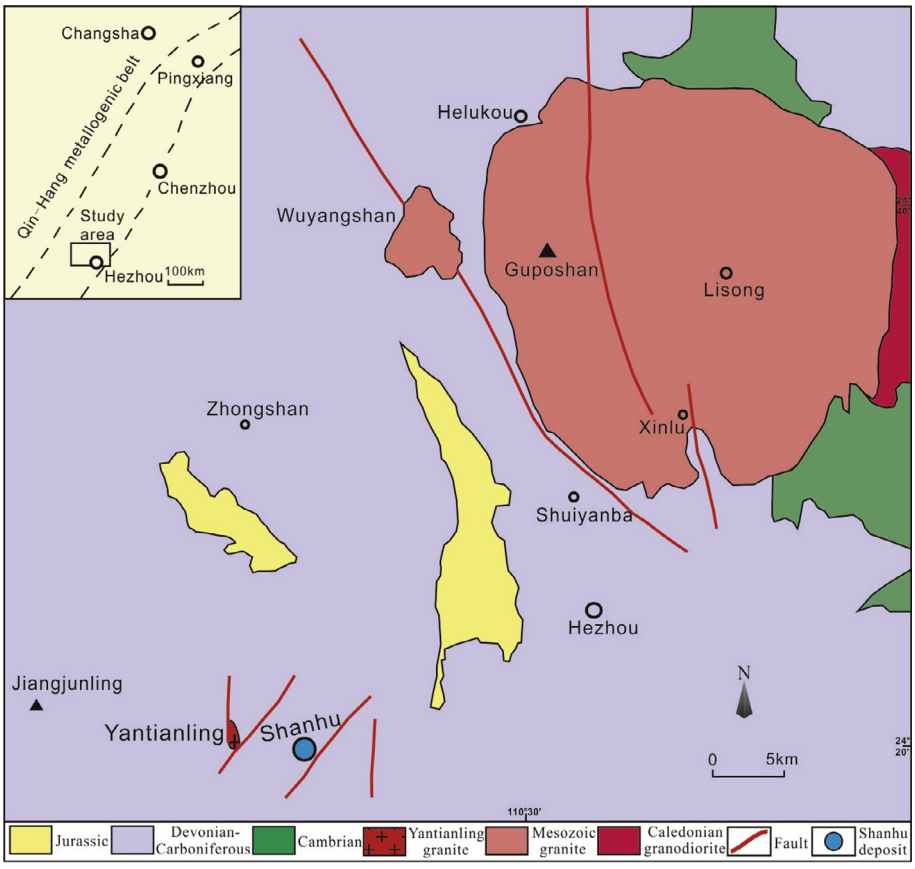

Fig. 2. Schematic geological map of the Shanhu orefield in the northeastern Guangxi Province.

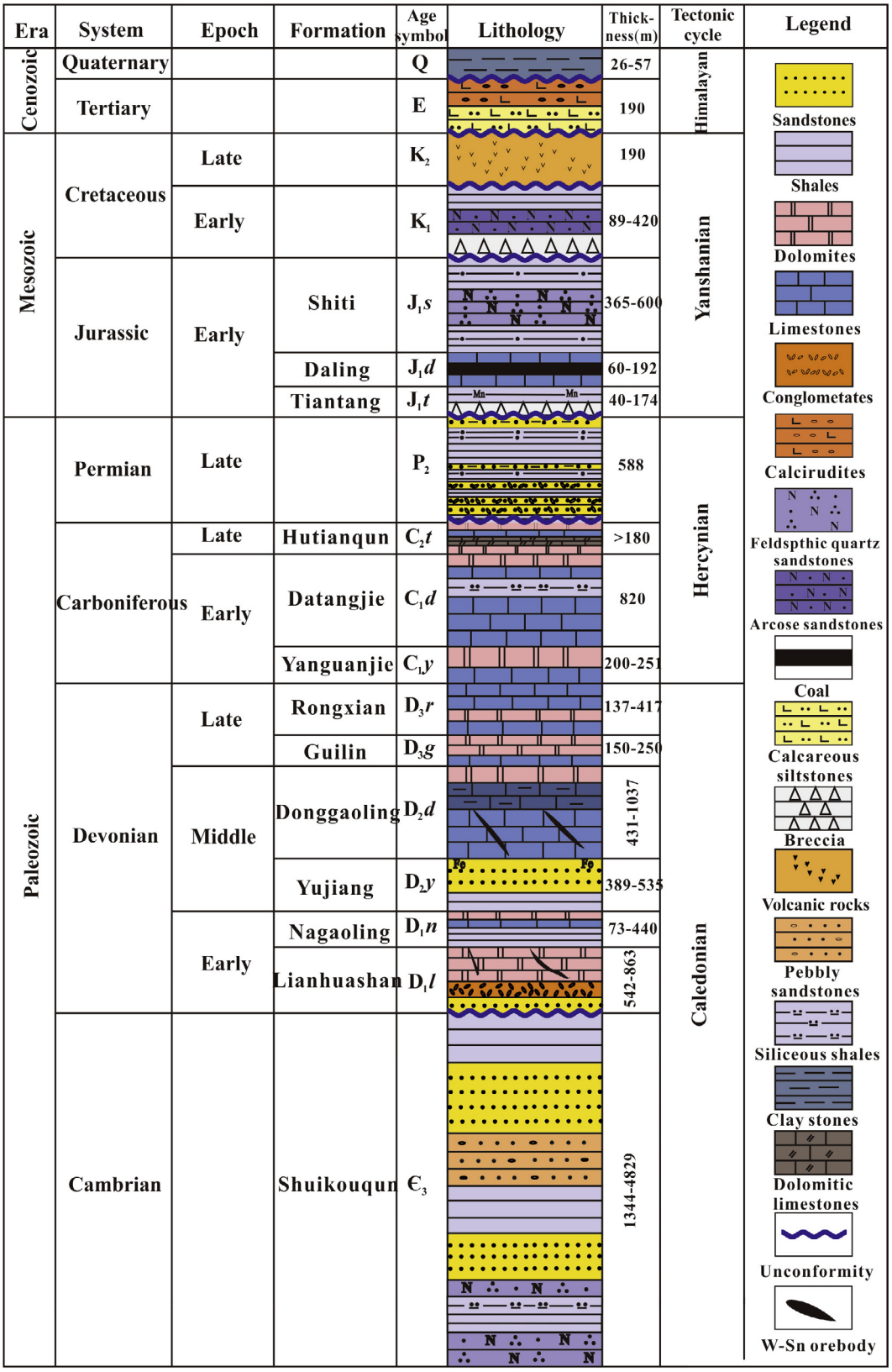

Fig. 3. Simplified stratigraphic column of the Shanhu orefield and its peripheral regions in the northeastern Guangxi, South China.

distributed in the northeastern Shanhu orefield (Fig. 2). Igneous rocks that outcrop in the Shanhu orefield are Yantianling granites. Underlying granites were inferred to exist in the region based on geophysical and remote sensing (Yang et al., 2007; Xiao et al., 2011). The Yantianling granite pluton was emplaced within Lower Devonian Lianhuashan Formation clastic rocks and has a surface exposure of approximately 0.14 km^2. The granite is white-gray in color and shows a porphyritic texture, in which the main minerals

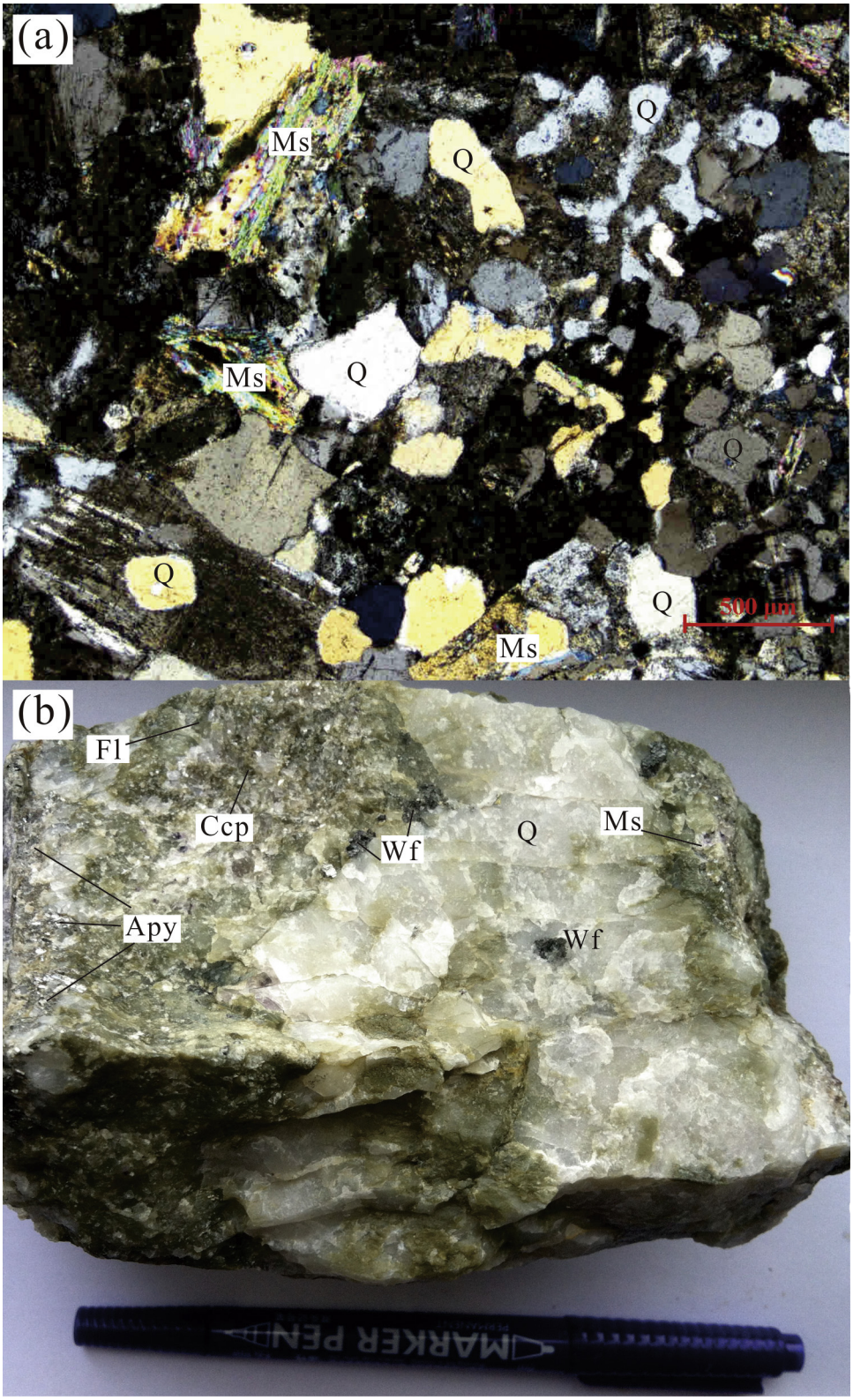

Fig. 4. Photomicrograph of the Yantianling granite (a), and photograph of the Shanhu orefield (b). Q: quartz, Wf: wolframite, Apy: Arsenopyrite, Ms: Muscovite, Ccp: Chalcopyrite, Fl: fluorite.

are quartz (~40%), sericite and muscovite (~55%) and feldspar (~2%) (Fig. 4a). Accessory minerals are fluorite, cassiterite, topaz, zircon, chalcopyrite, pyrite and sphalerite. Quartz is commonly anhedral with a length of 0.5–1 mm, and always encloses or replaces sericite and muscovite. The latter two minerals (i.e., sericite and muscovite) are white-gray and most of them are formed from the earlier orthoclase alteration. Feldspar grains are mostly anhedral and have always been altered to kaolinite.

Field observations show that hydrothermal alteration is common in the orefield, including silicification, muscovitization, sericitization, fluoritization, tourmalinization, carbonatization and chloritization, among which the muscovite, sericite and fluorite alteration are closely associated with W-Sn polymetallic mineralization (Fig. 4b). There are four different vein types in the Shanhu orefield, from east to west, including W-Sn quartz-vein, W-Sb fluorite-quartz vein, W quartz-breccia vein and Sn polymetallic sulfide. Among these, the W-Sn quartz-vein is the most important deposit type in the Shanhu orefield.

3. Sampling and analytical methods

The analyzed samples for zircon U-Pb dating were collected from Yantianling granite pluton (samples 15HZ38 and 15HZ40). The muscovite for Ar-Ar dating were extracted from quartz-vein type W-Sn ore (samples SH02 and SH08).

Zircon and muscovite grains were separated using standard magnetic and density methods from >2 kg samples and designed to minimize inter-sample cross-contamination. Following purification by hand sorting, and subsequently zircon grains were mounted in epoxy and polished down to near half sections to expose the grain interiors. Using a combination of optical microscopy and cathodoluminescence (CL), the clearest and least fractured rims of the zircon crystals were selected as appropriate targets for laser ablation analyses. Zircon U-Pb analyses were performed using a Laser ablation-multiple collector-inductively coupled plasma-mass spectrometry (LA-MC-ICP-MS) at the State Key Laboratory of Isotope Geochemistry, Guangzhou Institute of Geochemistry, Chinese Academy of Sciences (GIG, CAS). U-Pb ages were determined on samples 15HZ38 and 15HZ40. Sample mounts were placed in a two-volume sample cell flushed with Ar and He. Laser ablation was operated at a constant energy of 80 mJ and at 8 Hz, with a spot diameter of 30 μm. The ablated material was carried by He gas to the Aglient 7500a ICP-MS. Element corrections were made for mass bias drift, which was evaluated by reference to standard glass NIST 610 (Pearce et al., 1997). The zircon Temora was used as the age standard ($^{206}Pb/^{238}U$ = 416.8 Ma) (Black et al., 2003). $^{207}Pb/^{206}Pb$ and $^{206}Pb/^{238}U$ ratios were calculated using the ICPMSDataCal8.0 (Liu et al., 2008) and were then corrected using zircon 91,500 as the external standard. The $^{207}Pb/^{235}U$ ratios were calculated from the values of $^{207}Pb/^{206}Pb$ and $^{206}Pb/^{238}U$. Apparent U-Pb ages were computed by the Isoplot program (Ludwig, 2003).

Muscovite grains (~60 mesh) for Ar-Ar dating were collected and separated by carefully hand sorting from quartz vein-type W-Sn orebody (Fig. 4b) under a binocular microscope, then cleaned by ultrasonic bath of deionized water and acetone. Next, the samples were sealed into a quartz bottle for irradiation in a nuclear reactor at the Swimming Pool Reactor, Chinese Institute of Atomic Energy, Beijing. The total time for irradiation is 50 h, the neutron flux is about 6.0×10^{12} n cm^{-2} s^{-1}, and the integrated neutron flux is 1.13×10^{18} n cm^{-2}. The internal standard sample Fangshan biotite (sample ZBH-25, 132.7 ± 1.2 Ma, Wang, 1983) was also irradiated. The samples and monitors were heated in graphite furnace, and the heating-extraction step for each temperature increment was 30 min, with 30 min for purification. Analysis was performed at the ^{40}Ar-^{39}Ar Isotope Laboratory, Institute of Geology, Chinese Academy of Geological Sciences (CAGS), Beijing. The measured isotopic ratios were corrected for mass discrimination, blanks, atmospheric argon components and irradiation-induced mass interference. The correction factors of interfering isotopes produced during irradiation were determined by analysis of irradiated pure CaF_2 and K_2SO_4, yielding $(^{36}Ar/^{37}Ar)_{Ca}$ of 0.0002389, $(^{40}Ar/^{39}Ar)_K$ of 0.004782 and $(^{39}Ar/^{37}Ar)_{Ca}$ of 0.000806. The decay constant used for age calculation was $\lambda = 5.543 \times 10^{-10}$ a^{-1} (per year) (Steiger and Jager, 1977). All ^{37}Ar abundances were corrected for radiogenic decay (half-life 35.1 days). Data-processing were calculated using Isoplot program (Ludwig, 2003). Details of ^{40}Ar-^{39}Ar isotopic analytical method followed Zhang et al. (2006).

4. Analytical results

4.1. Zircon U–Pb geochronology

Zircons separated from samples 15HZ38 and 15HZ40 are generally euhedral to subhedral with length 100–250 μm and have aspect ratios ranging from 1:1 to 3:1. CL images exhibit strong oscillatory zoning with variable luminescence, indicative of igneous origin. The zircon U-Pb dating results are listed in Supplementary Table S1.

Sample 15HZ38: Twenty grains were analyzed, which have a relatively wide range of U and Th concentrations with U of 194–1347 ppm, Th of 103–1148 ppm and Th/U ratios in the range of 0.30–0.85 (Table S1). Twenty spots yield a coherent group with the $^{206}Pb/^{238}U$ weighted mean age of 100.9 ± 2.2 Ma with MSWD = 1.7 (Fig. 5a). In combination with the oscillatory zoning and Th/U ratios of the grains, this age can be interpreted as the formation age of the sample.

Sample 15HZ40: Sixteen analyses grains were carried out on this sample, and their U and Th concentrations range from 209 to 1199 ppm and 117–884 ppm, respectively, with Th/U ratios mostly in the range of 0.42 to 0.91. Sixteen spots yield a $^{206}Pb/^{238}U$

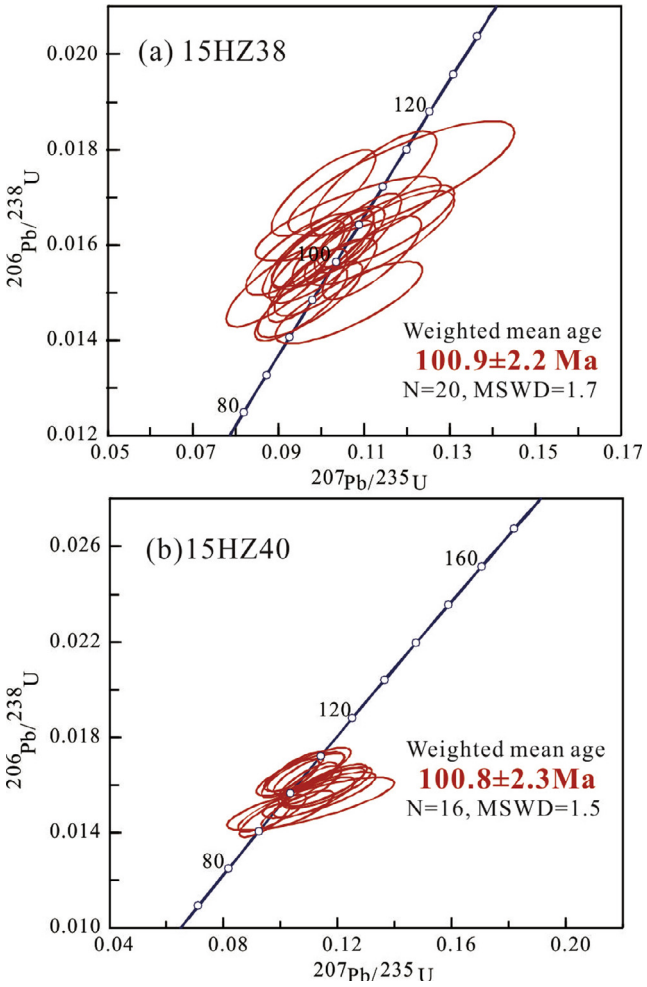

Fig. 5. Concordia diagrams showing LA-ICP-MS zircon analyses for the Yantianling granite.

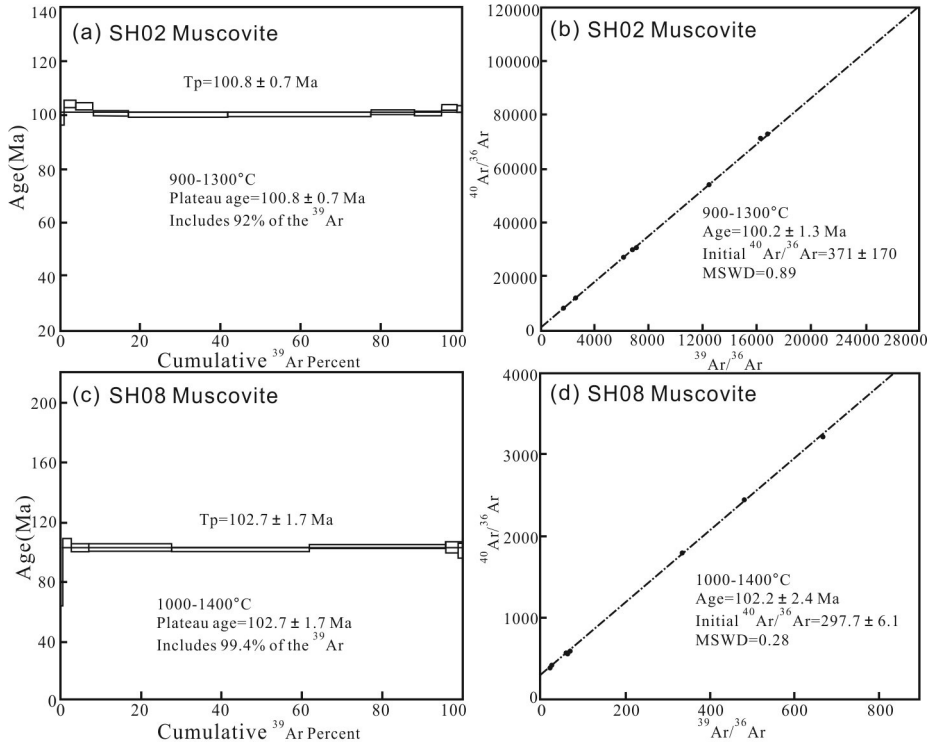

Fig. 6. Plateau and isochron ^{40}Ar-^{39}Ar age of muscovite from the Shanhu quartz vein W-Sn deposit.

weighted mean age of 100.8 ± 2.3 Ma with MSWD = 1.5 (Fig. 5b), representing the formation age of the sample.

4.2. Muscovite ^{40}Ar-^{39}Ar age

^{40}Ar-^{39}Ar analytical results are shown in Supplementary Table S2 and Fig. 6. Muscovite from sample SH02 was incrementally heated with 12 steps from 600 °C to 1300 °C, and yields a concordant age spectrum. The plateaus comprise 8 continuous steps accounting for 92% of the released total ^{39}Ar, and defined a plateau age of 100.8 ± 0.7 Ma (2σ). The isochron age of 100.2 ± 1.3 Ma (2σ, MSWD = 0.89) calculated from those 8 points coincides well with the plateau age. Muscovite from sample SH08 was performed by incremental heating with 10 steps from 700 °C to 1400 °C (Fig. 6). Seven continuous steps at temperatures of 1000–1400 °C are relatively coincident, and constitute a uniform and distinctly flat $^{40}Ar/^{39}Ar$ age spectra with 99.4% ^{39}Ar released. These steps yield a well-defined plateau age of 102.7 ± 1.7 Ma, an isochron age of 102.2 ± 2.4 Ma (2σ, MSWD = 0.28) at an initial $^{40}Ar/^{36}Ar$ ratio of 297.7 ± 6.1 (Fig. 6).

5. Discussion

5.1. Timing of granitic magmatism and W-Sn mineralization

Previous results showed that the emplacement age of the Yantianling pluton is controversial. For example, Liu (1989) reported a K-Ar age of 111–106 Ma for a greisenized granite sample from the Yantianling pluton. According to Rb-Sr isochron age analysis, however, Li et al. (1993) proposed that the Yantianling granite was emplaced at 148–137 Ma. In the same year, Wei et al. (1993) suggested that the Yantianling granite had Rb-Sr and K-Ar ages ranging from 137 Ma to 133 Ma. In contrast, our new precise age data for Yantianling granites yield zircon U-Pb ages of 100.9 ± 2.2 Ma and 100.8 ± 2.3 Ma, indicating that the Yantianling pluton was emplaced at ~101 Ma.

Muscovite ^{40}Ar-^{39}Ar dating is a very useful technique in determining the timing of hydrothermal mineralization particularly related to greisen or quartz vein (Snee et al., 1988; Selby et al., 2002). ^{40}Ar-^{39}Ar dating results in this study show that muscovites from quartz vein in the Shanhu orefield have ^{40}Ar-^{39}Ar plateau ages of 100.8 ± 0.7 Ma and 102.7 ± 1.7 Ma. In the Shanhu W-Sn polymetallic deposit, the muscovites are typically intergrown with cassiterite, arsenopyrite and fluorite (Fig. 4b), and the ^{40}Ar-^{39}Ar dating on muscovite shows good agreement between the plateau age and isochron age, within the applicable analytical errors. In addition, the initial $^{40}Ar/^{36}Ar$ ratios (297.7 ± 6.1, Fig. 6) in sample SH08 are well consistent with the atmospheric argon value (295.5 ± 5, Nier, 1950) within error and uncertainty, indicating absence of excess argon. Therefore, the plateau ages (100.8 ± 0.7 Ma, 102.7 ± 1.7 Ma) are believed as the crystallization age of the muscovite, and also represent the mineralization age of the Shanhu W-Sn polymetallic deposit, which are also coincident with the LA-ICPMS zircon U-Pb ages (100.9 ± 2.2 Ma, 100.8 ± 2.3 Ma) for the Yantianling granite. This fact suggests that the Shanhu W-Sn polymetallic deposit is temporally, spatially, and almost certainly genetically associated with the intrusion of the Yantianling granite. Therefore, we proposed that the intrusion of the granite and associated W-Sn polymetallic mineralization in the Shanhu mining area occurred at almost the same time (Late Cretaceous, ~101 Ma).

5.2. Episodes of Mesozoic W-Sn polymetallic mineralization in South China

The Mesozoic is the most important period of large-scale W-Sn polymetallic mineralization in South China (Pirajno, 2013a; Mao et al., 2013). Numerous recent high-precision geochronological data (Figs. 7 and 8, Also see Supplementary Tables S3–S5; Feng

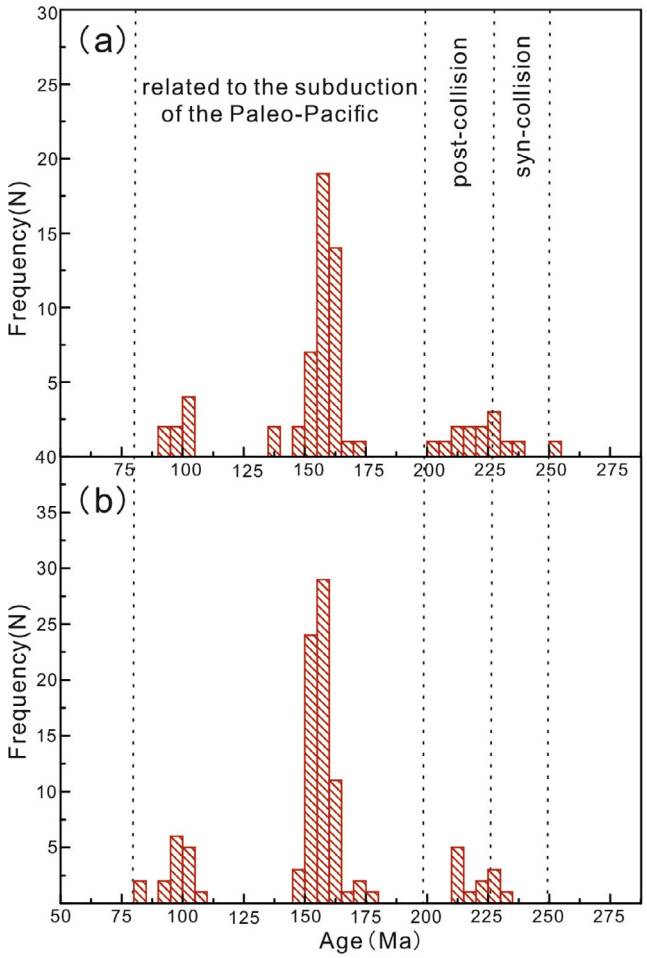

Fig. 7. Histogram of ages from the Mesozoic granites (a) and associated ore deposits (b) in South China. The age data are from Supplementary Tables S3–S5.

et al., 2015; Mao et al., 2013; Wu et al., 2015; Yuan et al., 2015; Zhou et al., 2015a) have shown that the Mesozoic polymetallic ore-forming processes can be divided into three episodes and phases, i.e., Middle-Late Triassic W-Sn-Nb-Ta mineralization (240–210 Ma), Middle-Late Jurassic W-Sn-Mo-Bi-Cu-Au-Ag mineralization (170–150 Ma) and Cretaceous W-Sn-Pb-Zn-Cu-Mo-Au-Ag mineralization (135–80 Ma).

The first episode of mineralization (240–210 Ma), sporadically distributed across eastern Guangxi (Limu, Liguifu, Yuntoujie and Gaoling deposits), southern Hunan (Yejiwo, Shuiyuanshan and Hehuaping deposits), southwestern Fujian (Hongshan deposit) and southern Jiangxi (Xian'etang deposit) provinces, is dominated by Sn, associated with W, Nb and Ta (Figs. 1, 7 and 8). Mineralization in this stage has been recognized in the past several years, and it can be classified as quartz vein-type, skarn-type and altered granite-type. Recently, more Middle-Late Triassic deposits have been reported in South China. However, most of them are middle to small scale and of no economic significance. One of the most famous deposits in this stage is the Limu W–Sn–Nb–Ta deposit (~214 Ma, Muscovite $^{40}Ar/^{39}Ar$ age, Feng et al., 2013; Yang et al., 2009) in northeastern Guangxi, South China, which is genetically associated with felsic and peraluminous leucogranites (~214 Ma, Zircon SHRIMP U–Pb age, Kang et al., 2012). These granites show a highly evolved fractionation sequence and are associated with distinct types of W-Sn-Nb-Ta mineralization (e.g., Zhu et al., 2001).

It is worth noting that earlier mineralization was remobilized by later tectono-magmatic events (Pirajno et al., 1997). In South China, some Triassic W–Sn ores and associated granitic rocks were overprinted by later Jurassic–Cretaceous granitic magmatism and their causative W-Sn mineral systems. For instance, the Xitian skarn Sn deposit in northeastern Hunan Province is usually considered of Jurassic age (~150 Ma, Muscovite $^{40}Ar/^{39}Ar$ age and Molybdenite Re–Os isochron age, Liang et al., 2016). However, field observations show that most of the orebodies are in the outer contact zone of the Indosinian granites (~230 Ma, Zircon SHRIMP U–Pb age, Fu et al., 2009). Recently, Zhou et al. (2015a) emphasize that the intrusion of the Indosinian granite in the Xitian deposit resulted in preliminary enrichment of ore-forming materials and formed massive skarns which were subsequently overprinted by the Late Jurassic granite pluton and the related Xitian large scale skarn W-Sn deposit.

The second episode of mineralization (170–150 Ma) is the most important phase in South China, resulting in three large-scale and high-grade W-Sn-Mo-Bi-Cu-Au-Ag polymetallic belts, which, from

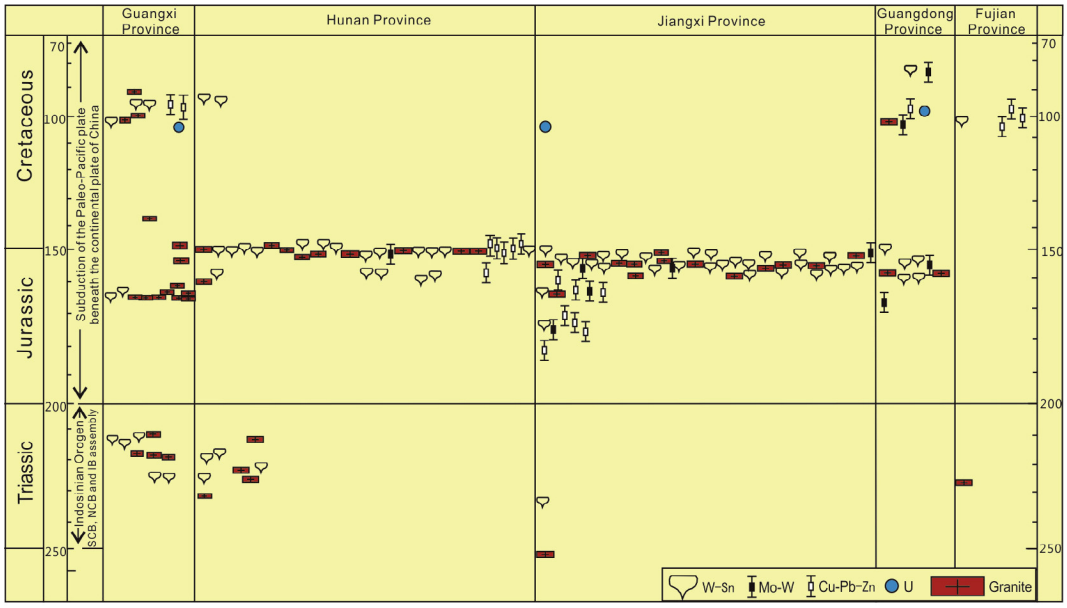

Fig. 8. Age range of Mesozoic granites and associated ore deposits in South China. Abbreviations: SCB, South China Block, NCB, North China Block, IB, Indochina Block. The age data are from Supplementary Tables S3–S5.

the northwest to southeast, are Middle–Lower Yangtze Valley metallogenic belt, Qin-Hang (Qinzhou, Guangxi Province to Hangzhou, Zhejiang Province) metallogenic belt and southeast coastal areas metallogenic belt. Two different types of mineralization are recognized along the three belts: (i) Cu-Au porphyry type mineralization and hydrothermal vein-type Pb–Zn–Ag and (ii) granite-related quartz vein-, skarn-, and minor greisen W–Sn–Mo–Bi mineralization. Granites related to the first type of mineralization fall in two age groups, i.e., 170–160 Ma and 140–130 Ma and show I-type signatures. The older group of granites are mainly distributed along the Qin-Hang metallogenic belt, whereas the younger group defines the Middle–Lower Yangtze Valley metallogenic belt. The second type of mineralization and associated granitic magmatism mainly occurred at 160–140 Ma, and more than 90% of W and Sn mineralization is related to this Jurassic and Cretaceous magmatism (Mao et al., 2013). This type of mineralization occurs predominantly in the Qin-Hang metallogenic belt and adjacent areas, and the mineral resources in these areas, from west to east, tend to decrease, whereas corresponding deposit types vary from skarn-type to quartz vein-type. Mao et al. (2013) propose that this is due to the fact that host rocks are characterized by dominant carbonate rocks in the west (southern Hunan and eastern Guangxi) and metaclastic rocks in the east (southern Jiangxi and northeastern Guangdong).

It is important to note that previous studies indicated that W-Sn mineralization was mainly related to S-type granite (Heinrich, 1990). However, some Jurassic granite plutons along the Qin-Hang metallogenic belt show A-type signatures (Zhou et al., 2015a). This suggests that W-Sn mineralization may not be limited to S-type granite, but also is related to A-type granite.

Our study shows that the Shanhu W-Sn polymetallic deposit has muscovite ^{40}Ar-^{39}Ar ages of 100.8 ± 0.7 Ma and 102.7 ± 1.7 Ma. Together with previous data, the results further suggest that Late Mesozoic (135–80 Ma) is another peak stage of W-Sn mineralization in South China (Figs. 7 and 8). This stage of mineralization is dominated by porphyry Cu, skarn Sn, U, associated with W, Mo, Au-Ag and Pb-Zn vein deposits. The porphyry Cu deposits are extensively distributed in the Middle–Lower Yangtze Valley metallogenic belt (~135–120 Ma, represented by Tongshankou Cu-Mo deposit in east Hubei Province, Dingjiashan Cu deposit in north Jiangxi Province and Dongguashan Cu-Au deposit in Aihui Province, Zhou et al., 2015d) and southeast coastal areas metallogenic belt (~105–95 Ma, represented by Zijinshan Cu-Au deposit in Fujian Province, Zhong et al., 2017; Yang and Wang, 2017). The skarn Sn deposits (~100–85 Ma), represented by Yanbei Sn deposit in Jiangxi Province, Yinyan Sn deposit in Guangdong Province, Dachang Sn deposit in Guangxi (Mao et al., 2013) and the Shanhu orefield in this study, are mainly distributed along the Qin-Hang metallogenic belt. In the southwestern part of Qin-Hang belt, hydrothermal U deposits are found in Xiangshan, Shazijiang and Xiazhuang areas with deposit ages in the range of 120–80 Ma.

In addition, ore-bearing porphyries (~149–105 Ma) in the Middle–Lower Yangtze Valley metallogenic belt are high-K calc-alkaline to calc-alkaline series, with the majority showing adakitic geochemical signature (Zhou et al., 2015d). They further proposed that these adakitic rocks may have originated from magma mixing. This indicates that mantle materials contributed to the formation of these porphyry Cu deposits.

5.3. Regional metallogenic implications

Early Mesozoic granites with an age range of 250–200 Ma are widely distributed in South China (Zhou et al., 2015b). Their intrusion was considered to result from the Triassic continental collision of the South China, North China and Indochina blocks (Faure and Ishida, 1990; Romer and Kroner, 2016). Zhou et al. (2006) further suggested that the Early–Middle Triassic (250–230 Ma) granites are syn-collisional, while the Late Triassic (220–200 Ma) granites are post-collisional. This is a possible reason why the former do not show related W-Sn mineralization, whereas the latter are mineralized with small deposits of skarns and quartz veins.

A series of recent studies proposed that the Late Mesozoic magmatism in South China resulted from the subduction of the Paleo-Pacific plate beneath the Eurasian plate based on regional tectonic evolution and geochronological and geochemical features of these igneous rocks (e.g., Jiang and Li, 2014; Li and Li, 2007; Pirajno, 2013b; Tang et al., 2014; Xia and Zhao, 2014; Mao et al., 2013; Zhou et al., 2015a,b; Romer and Kroner, 2016). Thus, the large scale of Late Mesozoic mineralization in South China was believed to be likely formed by the subduction of the Paleo-Pacific plate beneath the continental plate of China (e.g., Zhou et al., 2015a,b; Romer and Kroner, 2016; Deng et al., 2016).

In this study, our new precise zircon U-Pb and muscovite ^{40}Ar-^{39}Ar geochronological data show that the Yantianling granite and associated Shanhu W-Sn deposit were formed contemporaneously (103–101 Ma), implying a metallogenic event correlated to Late Cretaceous granitic magmatism in South China. The temporal-spatial consistency between Mesozoic granite evolution and mineralization in South China, and the distribution of a series of Late Cretaceous rift structures with red-bed sedimentary rocks (Wang and Shu, 2012) and volcanic-intrusive rocks (Zhou et al., 2015a), indicate that South China experienced a lithospheric extension during Late Cretaceous (Yuan et al., 2015; Zhou et al., 2015a and references therein). Thus, the emplacement of the Yantianling granite and associated W-Sn mineralization likely resulted from regional lithospheric extension during Late Cretaceous.

6. Conclusions

LA-ICPMS zircon U-Pb dating results show that the Yantianling granite yields an age of ~101 Ma, which corresponds well to muscovite ^{40}Ar-^{39}Ar age (103–101 Ma) of the associated Shanhu W-Sn deposit, indicating a spatial-temporal consistency between W-Sn mineralization and granitic magmatism. This provides convincing evidence for a Late Cretaceous mineralization event related to granitic magmatism in South China. Combined with regional tectonic, geochemical and geochronological data, it is suggested that the emplacement of the Yantianling granite and associated W-Sn mineralization likely resulted from lithospheric extension during Late Cretaceous.

Acknowledgements

We are grateful to the editor in-chief Prof. Franco Pirajno and two anonymous reviewers for their constructive and critical comments that helped significantly to improve the manuscript. We thank Lianhua Ma and Xiaoqiang Su for help with the maps. This study was supported by Key Programs of Higher Education of Guangxi Autonomous Region (KY2015ZD052), National Natural Science Foundation of China (41162005, 41502180, 41572191 and 41503021), Guangxi Natural Science Foundation Program (2015GXNSFDA139029 and 2015GXNSFBA139204), Postdoctoral Science Foundation of China for a funded project (2016M602550) to T. Shao and Guangxi Scientific Experiment Center for Mining, Metallurgy and Environment, Guilin University of Technology.

Appendix A. Supplementary data

Supplementary data associated with this article can be found, in the online version, at http://dx.doi.org/10.1016/j.oregeorev.2017.01.022.

References

Black, L.P., Kamo, S.L., Allen, C.M., Aleinikoff, J.N., Davis, D.W., Korsch, R.J., Foudoulis, C., 2003. TEMORA 1: a new zircon standard for Phanerozoic U-Pb geochronology. Chem. Geol. 200 (1–2), 155–170.

Cai, Y.F., Wang, Y.J., Cawood, P.A., Fan, W.M., Liu, H.C., Xing, X.W., Zhang, Y.Z., 2014. Neoproterozoic subduction along the Ailaoshan zone, South China: geochronological and geochemical evidence from amphibolite. Precambrian Res. 245, 13–28.

Cai, Y.F., Wang, Y.J., Cawood, P.A., Zhang, Y.Z., Zhang, A.M., 2015. Neoproterozoic crustal growth of the Southern Yangtze Block: geochemical and zircon U-Pb geochronological and Lu-Hf isotopicevidence of Neoproterozoic diorite from the Ailaoshan zone. Precambrian Res. 266, 137–149.

Chen, P.R., Hua, R.M., Zhang, B.T., Lu, J.J., Fan, C.F., 2002. Early Yanshanian post-orogenic granitoids in the Nanling region: petrological constraints and geodynamic settings. Sci. China 45, 755–768.

Cheng, Y.B., Mao, J.W., Chang, Z.S., Pirajno, F., 2013. The origin of the world class tin-polymetallic deposits in the Gejiu district, SW China: constraints from metal zoning characteristics and ^{40}Ar-^{39}Ar geochronology. Ore Geol. Rev. 53, 50–62.

Deng, J.H., Yang, X.Y., Li, S., Gu, H.L., Mastoi, A.S., Sun, W.D., 2016. Partial melting of subducted paleo-Pacific plate during the early Cretaceous: constraint from adakitic rocks in the Shaxi porphyry Cu–Au deposit, Lower Yangtze River Belt. Lithos 262, 651–667.

Faure, M., Ishida, K., 1990. The Mid-Upper Jurassic olistostrome of the west Philippines: a distinctive key-maker for the Palawan Block. J. Southeast Asian Earth Sci. 4, 61–67.

Feng, Z.H., Kang, Z.Q., Yang, F., Liao, J.F., Wang, C.Z., 2013. Geochronology of the Limu W-Sn- Nb-Ta-bearing granite pluton in South China. Resour. Geol. 63, 320–329.

Feng, C.Y., Zhao, Z., Qu, W.J., Zeng, Z.L., 2015. Temporal consistency between granite evolution and tungsten mineralization in Huamei'ao, southern Jiangxi Province, China: evidence fromprecise zircon U-Pb, molybdenite Re-Os, and muscovite ^{40}Ar-^{39}Ar isotope geochronology. Ore Geol. Rev. 65, 1005–1020.

Fu, J.M., Wu, S.C., Xu, D.M., Ma, L.Y., Cheng, S.B., Chen, X.Q., 2009. Reconstraint from zircon SHRIMP U-Pb dating on the age of magma intrusion and mineralization in Xitian ntungsten-tin polymetallic orefield, eastern Hunan Province. Geol. Miner. Resour. South China 3, 1–7 (In Chinese with English abstract).

Heinrich, C.A., 1990. The chemistry of hydrothermal tin(-tungsten) ore deposition. Econ. Geol. 85 (3), 457–481.

Jiang, X.Y., Li, X.H., 2014. In situ zircon U-Pb and Hf–O isotopic results for ca. 73 Ma granite in Hainan Island: implications for the termination of an Andean-type active continental margin in southeast China. J. Asian Earth Sci. 82, 32–46.

Kang, Z.Q., Feng, Z.H., Li, X.F., Liao, J.F., Yu, Y., Pan, H.B., 2012. ^{40}Ar-^{39}Ar age of muscovite in the Shuiyanba tungsen-tin ore field in northeast Guangxi and its geological significance. Bull. Mineral. Petrol. Geochem. 31 (6), 606–611.

Li, Z.X., Li, X.H., 2007. Formation of the 1300-km-wide intracontinental orogen and postorogenic magmatic province in Mesozoic South China: a flat-slab subduction model. Geology 35 (2), 179–182.

Li, R.K., Luo, L.Y., Li, S.Z., 1993. Guangxi tin deposits. Geol. Publishing House, 1–162.

Liang, X.Q., Dong, C.G., Jiang, Y., Wu, S.C., Zhou, Y., Zhu, H.F., Fu, J.G., Wang, C., Shan, Y.H., 2016. Zircon U-Pb, molybdenite Re–Os and muscovite Ar–Ar isotopic dating of the Xitian W–Sn polymetallic deposit, eastern Hunan Province, South China and its geological significance. Ore Geol. Rev. 78, 85–100.

Liu, K.H., 1989. Primary geochemical zoning of the Shanhu W-Sn deposit and its prospecting significance. J. Guilin Coll. Geol. 9 (4), 421–430.

Liu, Y.S., Hu, Z.C., Gao, S., Gunther, D., Xu, J., Gao, C.G., Chen, H.H., 2008. In situ analysis of major and trace elements of anhydrous minerals by LA-ICP-MS without applying an internal standard. Chem. Geol. 257 (1–2), 34–43.

Ludwig, K.R., 2003. User's manual for isoplot 3.0: a geochronological toolkit for Microsoft Excel. Berkeley Geochronol. Cent. Spec. Publ. 4, 1–71.

Mao, J.W., Cheng, Y.B., Chen, M.H., Pirajno, F., 2013. Major types and time-space distribution of Mesozoic ore deposits in South China and their geodynamic settings. Miner. Deposita 48, 267–294.

Nier, A.O., 1950. A redetermination of the relative abundance of the isotopes of carbon, nitrogen, oxygen, argon, and potassium. Phys. Rev. 77, 789–793.

Pearce, N.J.G., Perkins, W.T., Westgate, J.A., Gorton, M.P., Jackson, S.E., Neal, C.R., Chenery, S.P., 1997. A compilation of new and publishedmajor and trace element data for NIST SRM 610 and NIST SRM 612 glass reference materials. Geostand. Newsl. 21 (1), 115–144.

Pirajno, F., 2013a. Orogenic Belts: South China, Central China and Qinling-Dabie, Hinggan, The Geology and Tectonic Settings of China's Mineral Deposits. Springer, Dordrecht, Netherlands, pp. 249–380.

Pirajno, F., 2013b. Large Igneous Provinces (Xiong'er, Dashigou, 827 Ma Event, Tarim, Emeishan) and the Yanshanian Tectono-Thermal Event of Eastern China, The Geology and Tectonic Settings of China's Mineral Deposits. Springer, Dordrecht, Netherlands, pp. 547–638.

Pirajno, F., Bagas, L., Hickman, A.H., 1997. Gold mineralization of the Chencai-Suichang uplift and tectonic evolution of Zhejiang Province, southeast China. Ore Geol. Rev. 12, 35–55.

Romer, R.L., Kroner, U., 2016. Phanerozoic tin and tungsten mineralization-Tectonic controls on the distribution of enriched protoliths and heat sources for crustal melting. Gondwana Res. 31, 60–95.

Selby, D., Creaser, R.A., Hart, C.J.R., Rombach, C.S., Thompson, J.F.H., Smith, M.T., Bakke, A.A., Goldfarb, R.J., 2002. Absolute timing of sulfide and gold mineralization: A comparison of Re-Os molybdenite and Ar-Ar mica methods from the Tintina Gold Belt, Alaska. Geology 30, 791–794.

Snee, L.W., Sutter, J.F., Kelly, W.C., 1988. Thermochronology of economic mineral deposits: Dating the stages of mineralization at Panasqueira, Portugal, by highprecision $^{40}Ar/^{39}Ar$ age spectrum techniques on muscovite. Econ. Geol. 83, 335–354.

Steiger, R.H., Jager, E., 1977. Subcommission on geochronology: convention on the use of decay constants in geo- and cosmochronology. Earth Planet. Sci. Lett. 36, 359–362.

Tang, D.L.K., Seward, D., Wilson, C.J.N., Sewell, R.J., Carter, A., Paul, B.T., 2014. Thermotectonic history of SE China since the Late Mesozoic: insights from detailed thermochronological studies of Hong Kong. J. Geol. Soc. 171 (4), 591–604.

Wang, S.S., 1983. Dating of the Chinese K-Ar standard sample (Fangshan biotite, ZBH-25) by using the $^{40}Ar/^{39}Ar$ method. Sci. Geol. Sin. 4, 315–321 (In Chinese with English abstract).

Wang, D.Z., Shu, L.S., 2012. Late Mesozoic basin and range tectonics and related magmatism in Southeast China. Geosci. Front. 3, 109–124.

Wei, C.S., Xiong, C.Y., Liu, G.Q., 1993. Relation between structural deformation, dynamic evolution and metallization in Shanhu orefield, Zhongshan county, Guangxi. Guangxi Geol. 6 (4), 63–76.

Wu, S.H., Mao, J.W., Xie, G.Q., Geng, J.Z., Xiong, B.K., 2015. Geology, geochronology, and Hf isotope geochemistry of the Longtougang skarn and hydrothermal vein Cu–Zn deposit, North Wuyi area, southeastern China. Ore Geol. Rev. 70, 136–150.

Xia, S., Zhao, D., 2014. Late Mesozoic magmatic plumbing system in the onshore–offshore area of Hong Kong: insight from 3-D active-source seismic tomography. J. Asian Earth Sci. 96, 46–58.

Xiao, R., Li, X.F., Feng, Z.H., Yang, F., Song, C.A., 2011. ^{40}Ar-^{39}Ar dating of muscovite from tungsten-quartz veins in Shanhu tungsten-tin deposit and its geological significance. Miner. Deposita 30 (3), 488–496.

Yang, Y.F., Wang, P., 2017. Geology, geochemistry and tectonic settings of molybdenum deposits in Southwest China: A review. Ore Geol. Rev. 81 (Part 2), 965–995.

Yang, M.D., Huang, J., Cai, H.Y., 2007. Ore prospecting outlook of Sanhu tungsten-tin mine in Guangxi and its surrounding areas. Miner. Resour. Geol. 21 (2), 307–311.

Yang, F., Li, X.F., Feng, Z.H., Bai, Y., 2009. $^{40}Ar/^{39}Ar$ dating of muscovite from greisenized granite and geological significance in Limu tin deposit. J. Guilin Univ. Technol. 29, 21–24 (In Chinese with English abstract).

Yuan, S.D., Peng, J.T., Hao, S., Li, H.M., Geng, J.Z., Zhang, D.L., 2011. In situ LA-MC-ICP-MS and ID-TIMS U-Pb geochronology of cassiterite in the giant Furong tin deposit, Hunan Province, South China: new constraints on the timing of tin-polymetallic mineralization. Ore Geol. Rev. 43, 235–242.

Yuan, S.D., Mao, J.W., Cook, N.J., Wang, X.D., Liu, X.F., Yuan, Y.B., 2015. A Late Cretaceous tin metallogenic event in Nanling W-Sn metallogenic province: constraints from U-Pb, Ar-Ar geochronology at the Jiepailing Sn-Be-F deposit, Hunan, China. Ore Geol. Rev. 65, 283–293.

Zhang, Y., Chen, W., Chen, K.L., Liu, X.Y., 2006. Study on the Ar-Ar age spectrum of diagenetic I/S and the mechanism of 39Ar recoil loss-examples from the clay minerals of P-T boundary in Changxing, Zhejiang Province. Geol. Rev. 52, 556–561 (In Chinese with English abstract).

Zhong, J., Chen, Y.J., Pirajno, F., 2017. Geology, geochemistry and tectonic settings of the molybdenum deposits in South China: A review. Ore Geol. Rev. 81 (Part 2), 829–855.

Zhou, X.M., Sun, T., Shen, W.Z., Shu, L.S., Niu, Y.L., 2006. Petrogenesis of Mesozoic granitoids and volcanic rocks in South China: a response to tectonic evolution. Episodes 29 (1), 26–33.

Zhou, Y., Liang, X., Wu, S., Cai, Y., Liang, X., Shao, T., Wang, C., Fu, J., Jiang, Y., 2015a. Isotopic geochemistry, zircon U–Pb ages and Hf isotopes of A-type granites from the Xitian W–Sn deposit, SE China: constraints on petrogenesis and tectonic significance. J. Asian Earth Sci. 105, 122–139.

Zhou, Y., Liang, X., Kröner, A., Cai, Y., Shao, T., Wen, S., Jiang, Y., Fu, J., Wang, C., Dong, C., 2015b. Late Cretaceous lithospheric extension in SE China: constraints from volcanic rocks in Hainan Island. Lithos 232, 100–110.

Zhou, Y., Liang, X.Q., Liang, X.R., Jiang, Y., Wang, C., Fu, J.G., Shao, T.B., 2015c. U-Pb geochronology and Hf-isotopes on detrital zircons of Lower Paleozoic strata from Hainan Island: new clues for the early crustal evolution of southeastern South China. Gondwana Res. 27, 1586–1598.

Zhou, T.F., Wang, S.W., Fan, Y., Yuan, F., Zhang, D.Y., White, N.C., 2015d. A review of the intracontinental porphyry deposits in the Middle-Lower Yangtze River Valley metallogenic belt, Eastern China. Ore Geol. Rev. 65 (Part 1), 433–456.

Zhu, J.C., Li, R.K., Li, F.C., Xiong, X.L., Zhou, F.Y., Huang, X.L., 2001. Topaz-albite granites and rare-metal mineralization in the Limu District, Guangxi Province, southeast China. Miner. Deposita 36, 393–405.